International Journal of Science and Research Archive
eISSN: 2582-8185
Cross Ref DOI: 10.30574/ijsra
Journal homepage: https://ijsra.net/

(RESEARCH ARTICLE)

Check for updates

Structural Properties of Indium Tin Oxide (ITO) Deposited Thin Film Using Electron Beam Evaporation

Faruk Sani * and Hamza Yahaya

Department of Physics, Faculty of Physical and Computing Sciences, Usmanu Danfodiyo University, Sokoto, Nigeria.

International Journal of Science and Research Archive, 2025, 16(01), 1764-1769

Publication history: Received on 12 June 2025; revised on 24 July 2025; accepted on 26 July 2025

Article DOI: https://doi.org/10.30574/ijsra.2025.16.1.2220

Abstract

In this work, Indium Tin Oxide (ITO) thin films were deposited using electron beam evaporation on white glass substrates with different thin film thicknesses (50, 100 and 170 nm). The structural properties of the deposited samples were obtained using by X-ray Diffraction (XRD). The results showed that ITO thin films have a crystalline structure with a domain that increases in size with increasing thickness. The results showed that ITO thin films maintained the crystalline. That the highest nanoparticle size was obtained at the peak angle 30.84^{o} as 50.65 nm, 54.15 nm and 56.28 nm for the ITO samples deposited at 50 nm, 100 nm and 170 nm respectively. From the three ITO samples deposited, the ITO sample at 170 nm thickness exhibited the highest nano particle size while the lowest nanoparticle size was observed for ITO sample at 50 nm film thickness. These findings show the potential applications of ITO in optoelectronic and photovoltaic system.

Keywords: Electron Beam; Diffraction; Indium Tin Oxide; Thin Films; X-Ray

1. Introduction

Indium oxide doped with tin (In_2O_3 90%: SnO_2 10%) is briefly called ITO that is from the most famous transparent conductive oxides. Grown layers' completeness depends on the quality of interfaces which in turn depend on numbers of properties such as crystal structure and defects existence in thin film. In order to optimize above characteristics such as high transparency and low electrical resistance parameters such as thickness, doping type and level, and other conditions should be optimized. ITO has been specified optical property of conductive oxides such as In_2O_3 that heavily depends on caused imperfect density by external doping or their growth conditions. Originally, the addition of fluorine and tin atoms has been reported for external doping. ITO films have played an important role in deciding their characteristics and achieving highly crystalline and morphologically uniform thin films on flexible or suitable substrates for two applications. Also, ITO thin films find different applications include thin-film transistors, solar cells, organic light-emitting diodes (OLEDs), flat-panel displays, liquid- crystal displays, and plasma display panels light-emitting diodes (OLEDs), transparent electrodes, transparent heating elements, coating electrodes in optoelectronics instruments (flat panel displays (FPDs)), photovoltaic cells [1 – 8].

ITO thin films can be produced by different deposition techniques such as direct current (DC) and radio frequency (RF) magnetron sputtering although a variety of production methods have been used for making ITO films, for example electron beam evaporation, chemical vapor deposition, spray pyrolysis and reactive thermal evaporation. One of the techniques, important for studying physical and structural feature of thin films is X-ray reflectivity (XRR). Also, XRR is a highly efficient technique to research the structure of thin films from atomic scales to micrometer to obtain interface structures of thin film, density, thickness, and interfacial roughness. In the other word, the roughness of an interface is considered as a very important parameter in many industrial applications and quality of interfaces estimated by that. The ITO has proven to be an advanced semiconducting material opening a new window in many electronic and optical

* Corresponding author: Faruk Sani

Copyright © 2025 Author(s) retain the copyright of this article. This article is published under the terms of the Creative Commons Attribution License 4.0.

industries due to its large optical band gap and the plasma frequency lying in the near IR spectral region. Spray pyrolysis technique offers a simple and inexpensive experimental arrangement, ease of adding various doping materials, high growth rate and mass production capability for uniform large area coatings which are desirable for industrial applications. Although the dominant commercial market for laser glass is in large laser systems for inertial confinement fusion research with application to fusion energy and weapons physics science, these materials have also found their way into a number of industrial and laboratory environments. One leading application is in the field of laser shock peening. Structural characteristics of thin films are technologically very important. Characteristics of these films are necessary to design the films with required physical properties. [9] deposited SnO_2 thin films by Electrostatic Spray Deposition using $SnCl_2$ and ethanol on a Au-coated Pyrex glass substrate at 773 K. [10] deposited ZnO thin films using atom beam sputtering and their modifications have been shown by two processes: (a) thermal annealing of ZnO thin films in oxygen and (b) a thermal annealing by irradiation of these films by swift heavy ions (SHIs) in a high vacuum chamber. The as-deposited films showed the nanocrystalline nature with a preferred orientation along the c-axis of the hexagonal structure as revealed by x-ray diffraction (XRD) and Raman spectra. [11] reported a structural and optoelectronic properties of nanostructured ITO thin films deposited by chemical spray pyrolysis. [12] deposited a multilayer transparent conductive oxide film via radiofrequency magnetron sputtering. The authors found that the multilayer TCO structures have the potential to be more optically and electrically efficient in optoelectric devices performance. This research is aimed to further explore the structural properties of ITO thin films deposited by electron beam evaporation technique**.**

2. Materials and Method

Indium Tin Oxide (weight ratio; 90% In_2O_3 and 10% SnO_2), Glass substrates, measuring cylinder, Digital weighing balance, Beaker(200ml), Annealing machine, Syringe (1ml), quartz crystal microbalance, distilled water, and hydrogen peroxide.

2.1. Theoretical Equations Governing the Structural Analysis

Using the Scherer equation as shown in equation 3.1, the crystalline domain size (which can be equal t or smaller than the grain size) can be calculated from measurement of the observed x-ray diffraction peak.

$$D = \frac{K\lambda}{\beta Cos\theta} \quad \frac{K\lambda}{\beta Cos\theta} \qquad \text{..... 3.1}$$

where D represent crystalline domain size (nm), λ wavelength of the x-ray probe beam (0.15405nm), β is the peak width at half height (phase peak) in term of radian's, k is the shape of factor (approximately 0.94).

The material index of refraction in the x-ray region can be obtained from equation 3.2.

$$n = 1 - \delta + i\beta \qquad \text{..... 3.2}$$

where λ is the x-ray wavelength (λ = 1.54Å) and β = is the x-ray absorption length.

XRR critical angle is related to the effective electron density p by relation indicated in equation 3.3.

$$\theta_c\theta_c = \sqrt{2\delta}\sqrt{2\delta} = \lambda\sqrt{\rho \times r_e/\pi}.\sqrt{\rho \times r_e/\pi}. \qquad \text{..... 3.3}$$

Equation 3.3 is the resulting for external general reflection with control and with expansion to cosines

$$\alpha = \sqrt{2\delta}\sqrt{2\delta} = \frac{\sqrt{4\pi\rho r_0}\sqrt{4\pi\rho r_0}}{K \quad K}. \qquad \text{..... 3.4}$$

To measure the thickness according to Snell`s law for two consecutive peaks of the reflectivity curves.

$$\lambda = 2dsin\theta \quad \ldots\ldots\ldots \quad 3.5$$

where d is the thickness of film due to small angle approximately for Smell`s law ($\sin\theta \approx \theta$), then equation 3.5 can be reduced to equation 3.6.

$$\lambda = 2d\theta \quad \ldots\ldots\ldots \quad 3.6$$

3. Methodology

3.1. Substrate Cleaning

Substrate cleaning is the process of breaking the bonds between substrates and contaminants without damaging the substrates in thin film deposition process. Substrate cleaning is an important factor to get reproducible films as it affects the smoothness, uniformity, adherence and porosity of the films. In this work, the substrates were washed with detergent solution followed by rinsing the substrate with HNO for 20 minutes and then rinsed with distilled water, ethanol and acetone for 10 minutes. Finally, the substrates were dried in alcohol (methanol) vapors.

3.2. ITO Thin Film Deposition

Due to high melting point of Indium Tin Oxide (weight ratio; 90% In_2O_3 and 10% SnO_2), the electron beam evaporation method was used. The samples were placed in the vacuum chamber. The initial pressure was adjusted to 1×10^{-6} mbar while the partial pressure of the oxygen was regulated in stable amount 6.2×10^{-5} mbar. The film deposition was carried out in deposition rate 0.10 $nm \cdot s^{-1}$ to produce thin films with thicknesses of about 50, 100 and 170 nm. Film thicknesses were measured with a quartz crystal microbalance. The substrate temperature was kept constant at 400˚for 1 hour. Film thicknesses were measured with a quartz crystal microbalance.

3.3. Annealing

To improve ductility, recovery, recrystallization, and grain growth, annealing process was carried out. In this work, large ovens are used for the annealing process the inside of the oven is large enough to place the workpiece in a position to o receive maximum exposure to the circulating heated air. The samples were taken for structural characterization using X-ray diffraction machine.

4. Results and Discussion

4.1. XRD Results

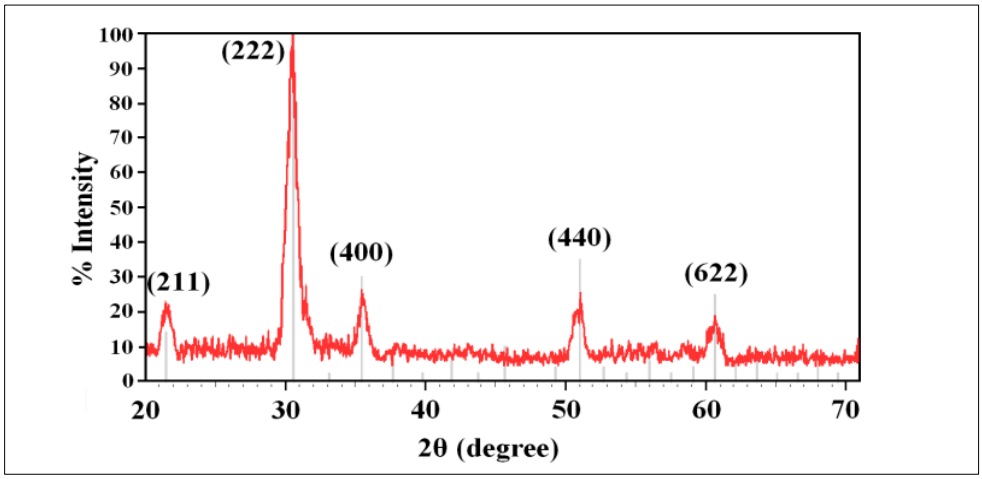

Figure 1 X-ray diffraction pattern of ITO thin film with deposition

The diffraction peaks at 2θ=21.88°,30.84°,35.81°,51.32°,60.96°, corresponding to (211), (222), (400) and (622) plane respectively were obtained. This can be indexed as the primitive cubic system by comparison with data from ITO (JCPDS No. 06-0416). Similarly, the average size of nanoparticle 20 to 34nm was obtained.

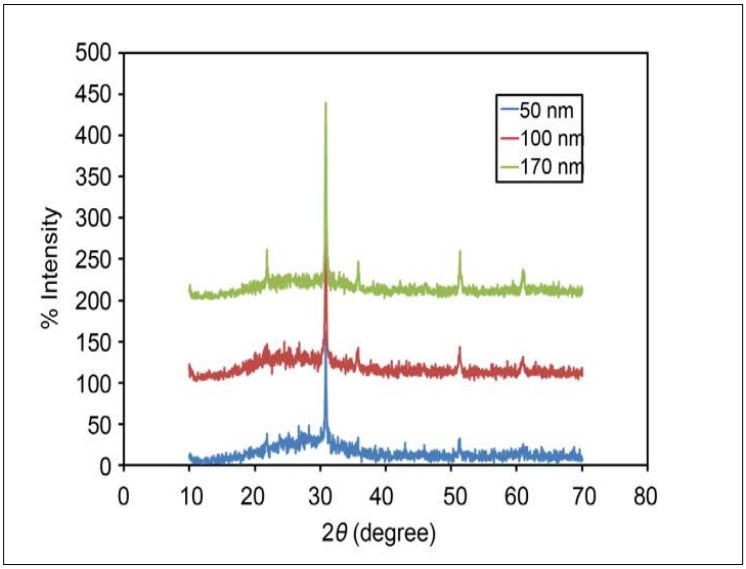

Figure 2 X-ray diffraction patterns of ITO thin films with for thicknesses of 50, 100 and 170 nm

It could be seen from Figure 4.2 that decreasing X-ray diffraction peaks with increasing thicknesses, corresponding to more regular crystalline structure.

Table 1 XRD of ITO thin film at thickness 50nm

Peak angle 2θ(deg)	FWHMB (rad)	FWHMB(^{o}C)	Nano particle size D(nm)
21.88	0.01713	0.982	8.60
30.84	0.00296	0.170	50.65
35.81	0.01135	0.651	13.40
51.32	0.01029	0.590	15.60
60.96	0.00861	0.494	19.49

Table 2 XRD of ITO thin film at thickness 100nm

Peak angle 2θ(deg)	FWHMB (rad)	FWHMB (deg)	Nano particle size D(nm)
21.88	0.02344	1.344	6.29
30.84	0.00277	0.159	54.15
35.81	0.01156	0.663	13.15
51.32	0.00889	0.510	18.05
60.96	0.01262	0.724	13.30

Table 3 XRD 0f ITO thin film at thickness 170nm

Peak angle 2θ(deg)	FWHMB (rad)	FWHMB (deg)	Nanoparticle size D(nm)
21.88	0.00493	0.283	29.87
30.84	0.00266	0.153	56.28
35.81	0.00669	0.384	22.71
51.32	0.00375	0.215	42.83
60.96	0.00791	0.454	21.21

Table 4 Calculation structural parameters of ITO thin film for thicknesses 50,100 and 170nm

Roughness (nm)	MED (e/Å^3)	Layer
10.2	5.1	50nm
10.7	5.1	100nm
9.3	4.8	170nm

It could be seen from The Tables 4.1, 4.2, and 4.3 that the highest nanoparticle size was obtained at the peak angle 30.84^o as 50.65 nm, 54.15 nm and 56.28 nm for the ITO samples deposited at 50 nm, 100 nm and 170 nm respectively. These nanoparticles obtained are within the range of the nanoparticles reported [11]. Conversely, lower FWHMB were observed for the three samples at the peak angle 30.84^o. The ITO sample at 170 nm thickness exhibited the highest nano particle size while the lowest nanoparticle size was observed for ITO sample at 50 nm thickness. This indicates that lower surface roughness can be achieved at ITO deposited at 50 nm thickness.

5. Conclusion

In this work, ITO thin films were deposited by electron beam evaporation on white glass substrates with varied thicknesses (50, 100 and 170 nm). The XRD was employed for the structural characterization. The results showed that ITO thin films maintained the crystalline. The highest nanoparticle size was obtained at the peak angle 30.84^o as 50.65 nm, 54.15 nm and 56.28 nm for the ITO samples deposited at 50 nm, 100 nm and 170 nm respectively. Among the three ITO film samples, the ITO sample at 170 nm thickness exhibited the highest nano particle size while the lowest nanoparticle size was observed for ITO sample at 50 nm thickness. Conclusively, these findings show the potential applications of ITO in optoelectronic and photovoltaic system.

Compliance with ethical standards

Disclosure of conflict of interest

The authors declare no conflict of interest.

References

[1] Xu, H.; Lan, L.; Xu, M.; Li, M.; Luo, D.; Xiao, P.; Peng, J. (2013). Low-Roughness and Easily-Etched Transparent Conducting Oxides with a Stack Structure of ITO and IZO. ECS J. Solid State Sci. Technol., 2, R245–R248.

[2] Lee, D.; Lee, A.; Kim, H.-D. (2023). IZO/ITO Double-Layered Transparent Conductive Oxide for Silicon Heterojunction Solar Cells. IEEE Access 2022, 10, 77170–77175. Coatings, 13, 1719 17 of 19

[3] Gonçalves, G.; Elangovan, E.; Barquinha, P.; Pereira, L.; Martins, R.; Fortunato, E. (2007) Influence of Post-Annealing Temperature on the Properties Exhibited by ITO, IZO and GZO Thin Films. Thin Solid Film, 515, 8562–8566.

[4] Raniero, L.; Ferreira, I.; Pimentel, A.; Gonçalves, A.; Canhola, P.; Fortunato, E.; Martins, R. (2006). Role of Hydrogen Plasma on Electrical and Optical Properties of ZGO, ITO and IZO Transparent and Conductive Coatings. Thin Solid Film, 511–512, 295–298.

[5] Jeong, J.-A.; Choi, K.-H.; Bae, J.-H.; Moon, J.-M.; Jeong, S.W.; Kim, I.; Kim, H.-K.; Yi, M.-S. (2009). Electrical, Optical, and Structural Properties of ITO Co-Sputtered IZO Films by Dual Target Magnetron Sputtering. J. Electroceramics, 23, 361–366.

[6] Sasabayashi, T.; Song, P.K.; Shigesato, Y.; Utsumi, K.; Kaijo, A.; Mitsui, A. (2001). Internal Stress of ITO, IZO and GZO Films Deposited by RF and DC Magnetron Sputtering. MRS Proc, 666, F2.4.

[7] Kim, S.M.; Park, S.J.; Yoon, H.H.; Choi, H.W.; Kim, K.H. (2009). Preparation of ITO and IZO Thin Films by Using Facing Target Sputtering (FTS) Method. J. Korean Phy. Soc., 55, 1996–2001.

[8] Morales-Masis, M.; Martin De Nicolas, S.; Holovsky, J.; De Wolf, S.; Ballif, C. (2015). Low-Temperature High-Mobility Amorphous IZO for Silicon Heterojunction Solar Cells. IEEE J. Photovolt, 5, 1340–1347

[9] Matsushima,Y.Nemoto,Y.Yamazaki,T.Maeda,K.and Suzuki,T.(2003). Pyrolysis method and the gas sensitivity for H2 Sens. Actuators B Chem, 961333e138

[10] Agrawal,S.Yamamoto, T. Yamanaka and Z. Ueda, J. (2008). Physics of very thin ITO conducting films with high transparency prepared by DC magnetron Sputtering,Thin solid films, 37-42.

[11] Al-hamdani, A.H. (2014). Structural and optoelectronic properties of nanostructured ITO thin films deposited by chemical spray pyrolysis techniques. Journal of materials science and Engineering B, 4(12), 346 –352, doi:10.17265/2161-6221/2014.12.002

[12] Seyhan, A. and Kartel, E. (2023). Optical, Electrical abd Structural Properties of ITO/IZO and IZO/ITO multilayer transparent conductive oxide films deposited via radiaofrequency magnetron sputtering. Coatings, 13(10), 1719, https://doi.org/10.3390/coatings13101719.